Experimental Study on Methane Desorption with the Coupling Effects of High Pressure Water and Thermal

Dong ZHAO[1], Dayuan LI[1], Yulin MA[2], Zengchao FENG[1,3], Yangsheng ZHAO*[1,3]

(1. College of Mining Engineering, Taiyuan University of Technology, Taiyuan, P.R.China; 2. School of Mechanics & Engineering, Liaoning Technical University, Fuxing, P.R.China; 3. Institute of Mining Technology, Taiyuan University of Technology, Taiyuan, P.R.China)

Corresponding Author: Yangsheng Zhao. **E-mail Address:** y-s-zhao@263.net

Abstract: Moisture and thermal are the key factors for influencing methane desorption during CBM exploitation. Using high pressure water injection technology into coalbed, new fractures and pathways are formed to methane transport. It is existed a phenomenon of water inhibiting gas flow. This study is focused on various water pressures impacted on gas adsorbed coal samples, then the desorption capacity could be revealed under different conditions. And the results are shown that methane desorption capacity was decreased with water pressure increased at room temperature and the downtrend would be steady until water pressure was large enough. Heating could promote gas desorption capacity effectively, with the increasing of water injection pressures, the promotion of thermal on desorption became more obvious. There are the others effects on methane desorption capacity influenced by water injection and thermal.

Keywords: methane; desorption; water injection; thermal

1 Introduction

Coalbed methane, CBM, is a significant natural energy resource and plays an important role in the structure of clean and new energy in China. However, currently, China CBM cannot satisfy requirements for effective and efficient recovery due to low permeability, low reservoir pressure and high gas adsorption capacity. (Zhou et al., 2016) With increased mining depth, ground stress, and gas pressure, as well as low gas permeability of coal seams, the gas extraction became difficult before mining. (Fu et al., 2007) The decrease in gas pressure during gas immigration can lead to gas desorption and cause matrix contraction, leading to fracture extension and further improving the permeability of the coal seam. (Li et al., 2016)

Furthermore, their permeability in the gas discharge process is complicated and can be affected by the coupled processes of gas migration and deformation of the coalbed. The mechanism of coupled flow and deformation on CBM recovery has drawn immense attention and significant achievements. (Chen et al., 2017) To increase coal seam permeability and reduce the amount of extraction drilling and risk of outburst, researchers studied techniques and methods of hydraulics. These methods include ordinary drill, enhanced drills, coalbed water injection, hydraulic punching, hydraulic cutting and hydraulic fracturing, they are widely used in modern coal mining to improve coalbed permeability and gas output. All these processes are including high pressure water. Thus, if high pressure water has been injected into coalbed, the desorption capacity of methane would be effected due to moisture. (Zhao et al., 2011)

Some researchers have engaged in this field in order to improve coalbed permeability and amount of gas output. The two major technologies are hydraulic fracture and thermal injection.

Hydraulic fracture will increase the moisture content in coalbed which it is resulting from water injection. According to the mechanism of moisture increased in coalbed, many scholars have performed studies on the influence of moisture on methane desorption (Xie et al. 2011; Zhang and Sang 2009), but they wet the coal samples before the experiment. Actually, after injecting water, the original equilibrium state of absorption and desorption will be broken. It makes very large differences between the experimental process and engineering practice. Therefore, it is very difficult to accurately explain the problems in engineering practice. Some scholars realized this problem (Pakowski et al. 2011; Xiao and Wang 2011; Zhang et al. 2011a; Zhao et al., 2011; Chen et al., 2015), and they perfected the experimental process in which water was injected into the dry coal samples under the equilibrium state of absorption methane. All of these results showed that the maximum desorption quantity decreases gradually with the amount of injected water, but they were not considering different water pressure impacted on same equilibrium adsorption state.

Thermal injection is an new technology in CBM exploitation, and they have been successfully applied to the enhancement of coalbed methane recovery. (Chen et al., 2010; Wang et al., 2015; Song et al., 2015; Lin et al., 2015; Shahtalebi et al., 2016.) Thermal simulation technologies, such as alternative or supplementary methods for the enhancement of gas production from unconventional reservoirs, have gained great

attention in recent years. For example, electromagnetic materials, hot water injection, hot gas injection and microwave or radio have been used (Yahya et al., 2012; Salmachi and Haghighi, 2012; Bahrami et al., 2012). Methane desorption rate would be improved by coalbed heating, but the injected water could block the channels of gas flow imposing additional resistance on the transport and production of coalbed methane. Hot gas injection method would induce a binary gas flow and make the forecasting of gas production more difficult.

In this paper a proposal about thermal and water injection technology to improve coalbed methane production has been proposed. Combining high pressure water will block gas desorption and heat will accumulate gas output, a series experiments of methane bearing coal samples with water injection at different water and gas pressure. And then, heating coal samples after desorption of water injection. After that, desorption capacities of coal samples at different water injection pressure and thermal effects have been illustrated. The experiments on constant and warming temperature of desorption character of gassy coal under different water injection pressures were carried out. These results are expected to provide a clearer understanding of theoretical efficiency of heat water or steam injection into coalbed, they can provide some theoretical and experimental guidance on CBM production and methane control.

2 Methods

2.1 Coal samples and preparation

Coal samples used in experiments were taken from Gucheng and Gaohe Coal Mine

which were belong to No. 3 coal seam of Qinshui Coalfield in Lu'an Mining Area. Large coal samples were taken from the well and wax sealed on site. After reaching the laboratory, they were processed into $\Phi100mm\times100mm$ cylindrical specimen. The picture of experimental coal samples is shown in Fig. 1, the results of proximate and reflectance analysis are shown in Table 1.

Fig.1   Experimental apparatus and coal samples used in these experiments

Table 1   Analysis results of experimental coal

The samples are lumpy, which contained similar pores and fractures to a coal bed. Pores are the dominant place for gas storage and fractures for gas transportation. Methane adsorbed on the coal samples was used for CBM in situ, and enclosed CBM was simulated using water injection after adsorption.

2.2 Experimental apparatus

To study the adsorption/desorption characteristics of coal mass samples and to carry out simulated water injection CBM experiments, we constructed a new experimental system. The set-up comprises a stainless steel container that withstands pressures up to 20 MPa and has top and bottom openings with flexible seals. The top part is used to inject and produce gas and the bottom part is used to inject water. A columnar coal sample is placed inside the container, which is surrounded by a temperature-controlled air bath. Water injection and gas production in the apparatus are similar to the one water injection well per gas production well configuration under ideal conditions. The coal mass samples simulate an ideal coal bed after hydro-fracture. Gas usually desorbs rapidly, but once water is injected the process

slows down and becomes less efficient. A series of experiments was performed at different water pressures to determine the desorption behavior. The appearance and the schematic diagram of experimental apparatus are shown in Fig.1 and Fig. 2, respectively.

Fig.2   Schematic diagram of experimental apparatus used in this study

The gas system indicates the gas flow path and the liquid system provides introduces water at different pressure into gas-bearing samples. The system is controlled based on experimental conditions, including pressure and flow. Needle valves (V1, V2, V3) and gauges (G1, G2, G3) are used to regulate and show the pressure of methane (CH_4), helium (He) and water, respectively, and flow meters (F1, F2) are used to read the gas and liquid flow rate. In addition a switch valve (S1) is used to switch from methane to helium. Methane, the major CBM component, is supplied from a high-pressure cylinder (C1). Helium from cylinder C2 is used to check for leaks and measure free volume after sample in container. Then the helium was purged using a vacuum pump (M2) until the sample column contained no gas before methane injection. It will last more than 48h.

After testing for leaks and methane injection (the equilibrium pressure is shown on G5), liquid water was injected from the bottom until the container was full of water. This process simulates an ideal coal bed by injecting water around the surface of broken coal at a certain pressure. An injection device (M1) is used to inject liquid water. The injected water was left in place for approximately 24 h to simulate ideal water-bearing coal after hydro-fracture.

A control device (M3) was used to regulate the temperature via an air circulation system. The system for measuring water outflow consisted of a conical measuring flask to measure the flow volume during desorption. A gas collection system (M4), using displacement of water and a rotor flowmeter, was used to precisely determine the volume of desorbed methane (precision ±2 mL).

2.3 Experimental procedures

During the experiments, the coal samples were placed in adsorption-water injection-desorption apparatus at a room temperature of 25℃ which means coal reservoir temperature, and after up to 90℃ which is experimental temperature controlled by a temperature controller using thermal air flow. Before experiments began, the free volume of coal in container is measured. The experimental procedures are divided into three steps.

The first is the adsorption, checking the airtightness of the experimental device by the method of high-pressure helium, and then keep the device vacuum under airtightness more than 48h, finally open the valve for connecting gas container with sample container so that coal sample could be adsorbed gas, the process would last about 3 to 7 days until the gas pressure is constant. Under the rated adsorption pressure and the pressure change during the adsorption process is recorded by the digital pressure gauge.

The second is the high pressure water injection, connecting M1 to M3 after coal sample adsorption reached an equilibrium state. The water pressure is controlled by water pump in M1 and divided into four different pressures. They are water pressure

equal gas pressure (1 time), 2.5 times of gas pressure (2.5 times), 6.25 times of gas pressure (6.25 times) and 16 times of gas pressure (16 times). For contrast, natural desorption without water injection after adsorption is necessary. During water injecting process, water has run through the entire coal sample. Then kept the state of water in coal sample container for 24h. This process is simulated to moisture injection in the situ-coal seam.

The third is the desorption, it is separated two different steps. The one is room temperature desorption and the other is heating to 90℃ for desorption. M4 is connected to M3 for desorption under atmospheric pressure. The desorption process of desorption would last 48h in each experiment and the desorption gas is collected. The amount of gas desorption is measured in real time during the experiment and after less than 10ml/h, it is considered that the desorption equilibrium has been reached.

3 Experimental results

3.1 Raw data of experiments

Table 2 and Table 3 showed the raw data of adsorption, water injection and desorption of the coal sample, in which 1#,2# and 1_2# coal samples represent desorption of Gucheng coal sample at 25℃, desorption of Gaohe coal sample at 25℃ and desorption of Gucheng coal sample at 90℃, respectively. The definitions of parameters in the table are shown in Table 2. The data of gas adsorption pressure around 0.25 MPa and 0.5 MPa are shown in Table 2 and Table 3, respectively.

Table 2   Raw data of the two coal samples at gas adsorption pressure around

0.25MPa

Table 3　Raw data of the two coal samples at gas adsorption pressure around 0.50MPa

3.2 Analyses for experimental results

3.2.1 Results of desorption at 25℃ and 90℃

Curves of desorption capacity versus time in different water injection pressure for the two coal samples at adsorption pressure around 0.25 MPa and 0.50MPa are shown in Fig.3 and Fig.4,respectively. The desorption stage of coal sample 1# had separated into two stages which the first is 25℃ and the second is 90℃, the two stages are continuous. And the stage of coal sample 2# only had one just 25℃ desorption. The results of the two samples could be contrasted with different desorption stages.

Fig.3　Desorption capacity versus time in different water injection pressure at 0.25MPa gas adsorption pressure

Fig.4　Desorption capacity versus time in different water injection pressure around 0.50MPa gas adsorption pressure

As shown in Fig.3, under the condition of room temperature of 25℃, the desorption percentage of adsorption gas is increased with time rapidly. (**Desorption percentage** is the proportion of desorption gas and whole adsorbed gas in real time) The instantaneous desorption rate of all the experiments reaches the final desorption rate of 71.53% in 500 minutes. The instantaneous desorption rate of gas after injection is not obvious with time increase, the data in slowly growth with time. The larger the

injection pressure, the more difficult it is to desorb, the lower the final desorption percentage.

In the same coal sample, with the increase of adsorption pressure, whether in natural desorption or water injection desorption, the final gas desorption percentage of sample has been improved to some extent. When using 2 times of former adsorption pressure in Fig.4, desorption percentage of Gucheng and Gaohe coal samples increased by 11.44% and 27.82% in Natural desorption. Water injection pressure is higher, the increase of adsorption pressure on gas desorption rate is more obvious in water injection desorption. Under 16 times of water injection pressure, contrast with 0.25 MPa gas pressure, and the desorption percentage of Gucheng and Gaohe coal samples increased by 2.473 times and 2.047 times, respectively.

When the temperature rises to 90℃, the Gucheng coal sample showed a significant increase in the desorption rate of coal methane compared with 25℃ when water injection pressure and adsorption pressure are constant. The final desorption percentage at 90℃ increased by 1.331 times compared with that at 25℃ in natural desorption. With the increase of water injection pressure, the effect of heating on desorption rate increased significantly. At 16 times of water injection pressure, thermal promotes the desorption and the gas desorption rate increased by 10.72 times which is compared to room temperature. This is shown that thermal could enhance the ability of coal methane desorption effectively, and inhibition effect of water injection was weaken.

The time effect of desorption in the process of mining coalbed methane is a very

important indicator, which is the direct influence factor of the recovery efficiency. Therefore, based on the description of the desorption capacity of coalbed-methane with the change of time, the paper (Zhao et al., 2011) uses the following formula to analyze the relationship between desorption rate and time under different conditions:

$$\eta = \eta_{max}\left\{1 - \exp\left[-\left(\frac{t}{t_0}\right)^n\right]\right\}$$

(1).

In this formula, t_0 and n were the desorption median time parameters and the time effect of divergence; t is the time. The above parameters are related to experimental water pressure and type of coal.

Equation (1) is transformed and can be changed to (2) if $x = t$

$$y = \left(\frac{x}{t_0}\right)^n$$

(2).

According to Equation (1) and (2), a regression analysis has been made using the experimental results, the simulation results is shown in Table 4. It can be seen that the time-dependent parameter t_0 of desorption gradually increases with the change of water injection pressure, which indicates that high pressure water injection will affect the desorption rate of coalbed methane.

Table 4   Simulation results of time effect on desorption

3.2.2 The relationship between final desorption percentage and water injection pressure

Desorption capacity as a function of water pressure for the two coal samples at 0.25 MPa and 0.50 MPa gas adsorption pressure are shown in Fig.5 and Fig.6, respectively. From natural desorption to 2.5 times water injection pressure and then

6.25 times water injection pressure, the desorption percentage is a gradual change in the slope of the curve, and the data change of water pressure from 6.25 times to 16 times is small and relatively straight. With the increase of multiples of injection pressure, the impact of water injection on the desorption rate is initially severe, and then gradually slows down, and finally approaching an equilibrium state. With the adsorption pressure became greater, the desorption percentage raised for same type of coal samples. This is due to the adsorption of gas has the greater desorb potential energy and the stronger ability to breakthrough constraint of capillarity for adsorption equilibrium pressure of coal samples so that the coal samples have stronger desorption capacity.

Fig.5   Desorption capacity as a function of water pressure for the two coal samples at 0.25MPa gas adsorption pressure

Fig.6   Desorption capacity as a function of water pressure for the two coal samples at 0.50MPa gas adsorption pressure

To reveal the final desorption percentage of natural desorption and four different water injection pressures, according to isothermal adsorption-desorption formula, one transformation of it could be introduced in basis of experimental results between the desorption rate and water pressure.

$$\eta_{max} = \eta_{d\,max}\left(1 - \frac{aP_2}{1 + bP_2}\right) \tag{3.}$$

In the expression, η_{dmax} is the final desorption percentage (%) of coal sample during natural desorption; a and b are related parameters (MPa^{-1}).

Equation (3) can be changed into the following form if $y = \dfrac{\eta_{d\,max}}{\eta_{d\,max} - \eta_{max}}$, $x = \dfrac{1}{P_4}$

$$y = \frac{1}{a}x + \frac{b}{a} \tag{4}.$$

Regression analysis of experimental results and simulation results are shown in Table 5 that *b/a* is one of the important indexes to measure the effect of water injection on gas desorption and the lower limiting value is 1, indicating that the gas desorption rate is equal to 0 when the water pressure is infinite. The value of *b/a* is close to 1 in this paper, indicating that the desorption rate of gassy coal will be decrease with the increase of external moisture injection pressure. The desorption rate will be close to zero when the water pressure increases to a certain value.

Table 5   Simulation results between desorption percentage and water injection pressure

The influence of moisture on coal desorption based on coal moisture content by using small particle size coal samples had been reveal in following forum (Wang et al., 2010):

$$\eta_d = \eta_{d\,max}\left(1 - \frac{0.032M}{1 + 1.152M}\right) \tag{5}.$$

In the expression, M is the water content (%).

This formula is similar to this article. The water content of coal is positively correlated with the water injection pressure and can be approximated by comparison, but the value of b/a that obtained is larger, indicating that the desorption rate is still about 4/5 at natural desorption when reaching saturated water content. The smaller the particle size of coal samples are, the less impact of external water injection on the

desorption of coal is.

4 Discussion

The essence of gas drainage is the conversion process of gas from adsorption to free state , and this process must involve two physical quantities which are gassy potential and chemical potential produced by coalbed-methane adsorption. The matter always tends to transform from a state with high chemical potential to a low one. Both reducing the pressure and increasing the temperature reduce the chemical potential of the free gas, which is favorable for the gas to be converted from the adsorbed state to the free state. Gas adsorption potential is to reflect the coal surface adsorption capacity of the methane. The larger the adsorption potential energy is, the less it is easily desorbed. And the higher the temperature is, the lower the adsorption potential energy is. In view of this, adsorption pressure and desorption temperature are inevitably important factors that affecting the gas from adsorption to free state transformation. Desorption capacity as a function of water pressure at 90℃ for coal sample 1# is shown in Fig. 7. Temperature has a promote effect on gas desorption, it is different from various water injection pressure.

Fig.7　Desorption capacity as a function of water pressure at 90 ℃ for coal sample 1#

On the other hand, 80% -90% of the methane in the actual coal seam is occluded in the pores and fissures of the coal body in the adsorbed state. Therefore, the pores and fissures are also the important factors that affect the gas desorption. The main

factors of the conditions of coal seam and pore is moisture in the actual coal mine production. In summary, the pressure, temperature and pore fissures are the key conditions for studying methane desorption. In this paper, the above conditions are studied by changing adsorption pressure, desorption temperature and multiples of injection pressure. In these experiments, coal samples became wet state after desorption in different water injection pressure. The mass of coal sample as a function of water pressure after desorption for coal sample 2# is shown in Fig.8. The moisture in samples is the dominating role for mass increasing.

Fig.8   Mass of coal sample as a function of water pressure after desorption for coal sample 2#

The larger adsorption pressure it has, the greater desorption pressure it will reduce and it will be more favorable to the release of chemical potential energy and will get higher the desorption rate. In this paper, 0.2MPa adsorption pressure desorption rate was significantly higher than 0.1MPa adsorption pressure. The heating process of Gucheng coal samples is very significant that the process of heating is promoted the desorption. In this paper, it can be seen from the research of different moisture injection pressure conditions that the desorption rate is getting lower and lower with the increase of moisture injection pressure because the moisture molecules obviously block the pores and cracks in the coal through water injection and the amount of desorption energy of the molecule greatly increases so the greater the pressure of water injection, the more difficult it is for the gas in the pore fissure to desorb. Throughout all the experiments, it can be confirmed that moisture injection

can effectively suppress gas desorption process.

5 Conclusion

In this paper, based on the desorption characteristics of gas-bearing coal under different conditions, a lot of the corresponding experiments has been done. We got the change regulation of desorption characteristics of gassy coal which was under different moisture injection pressure, different adsorption pressure and different temperature. The results are shown that:

The samples of Gucheng and Gaohe coal samples under adsorption pressure around 0.25MPa and 0.50MPa have different desorption capacity with different water injection pressure, 2.5, 6.25 and 16 times water injection conditions are 32.79%, 16.59% %, 11.94%, 5.29%; 46.66%, 24.03%, 17.26%, 9.29% (Gucheng); 56.01%, 17.33%, 7.32%, 0.94%; 52.07%, 22.27%, 15.76%, 12.76% (Gaohe).

Heating can effectively promote gas desorption, and with the increase of water injection multiples, the promotion of heating on the desorption more obvious. For the desorption rate in heating, equal pressure water injection,2.5, 6.25 and 16 times water injection increased about 6 times, 6 times, 7 times and 21 times respectively.

There is a certain time-median effect on the desorption of coal gas along with time after water injection, and it will vary with the water injection pressure. Under different water injection pressures, the final desorption rate of coalbed-methane under different moisture injection pressures and natural desorption under the same conditions have a certain functional relationship.

Acknowledgement

This study was supported by the National Natural Science Foundation of China (Grant Nos. 51304142 and 21373146) and by the Program for Outstanding Innovation Teams of Higher Learning Institutions of Shanxi (Grant Year 2014).

References

Bahrami, H., Rezaee, R., Clennell, B., 2012. Water blocking damage in hydraulically fractured tight sand gas reservoirs: an example from Perth Basin, Western Australia. J. Petrol. Sci. Eng. 88, 100-106.

Chen, S.K., Yang T.H., Ranjith P.G., Wei C.H., 2017. Mechanism of the Two-Phase Flow Model for Water and Gas Based on Adsorption and Desorption in Fractured Coal and Rock. Rock Mech Rock Eng. 50, 571-586.

Chen X.J., Chen Y.P., 2015. Influence of the injected water on gas outburst disasters in coal mine. Nat Hazards, 76, 1093-1109.

Chen, Z.W., Liu, J.S., Elsworth, D., Connell, L.D., Pan, Z.J., 2010. Impact of CO_2 injection and differential deformation on CO_2 injectivity under in-situ stress conditions. Int. J. Coal Geol. 81, 97-108.

Fu J.H., Cheng Y.P., 2007. The coal and gas outburst situation and prevention solutions in China coal mine. Mining and Safety Engineering Journal, 24, 253–259.

Li Y., Chen Y.F., Zhou C.B., 2016. Effective stress principle for partially saturated rock fractures. Rock Mech Rock Eng, 49, 1091–1096.

Lin, Y., Wang, H.Y., He, S., Nikolaou, M., 2015. Increasing shale gas recovery through thermal stimulation: analysis and an experimental study. SPE Annu. Tech. Conf. Exhib. 28-30. SPE 175070.

Liu Q, Cheng Y, Zhou H, Guo P, An F, Chen H (2014) A mathematical model of coupled gas flow and coal deformation with gas diffusion and Klinkenberg effects. Rock Mech Rock Eng 48:1163–1180.

Pakowski Z., Adamski R., Kokocin´ska M., 2011. Generalized desorption equilibrium equation of lignite in a wide temperature and moisture content range. Fuel, 90, 3330–3335.

Salmachi, A., Haghighi, M., 2012. Feasibility study of thermally enhanced gas recovery of coal seam gas reservoirs using geothermal resources. Energy & Fuels 26 (8), 5048-5059.

Shahtalebi, A., Khan, C., Dmyterko, A., Shukla, P., Rudolph, V., 2016. Investigation of thermal stimulation of coal seam gas fields for accelerated gas recovery. Fuel 180, 301-313.

Song, Y., Cheng, C., Zhao, J., Zhu, Z., Liu, W., Yang, M., Xue, K., 2015. Evaluation of gas production from methane hydrates using depressurization, thermal stimulation and combined methods. Appl. Energy 145, 265-277.

Wang, H., Merry, H., Amorer, G., Kong, B., 2015. Enhance hydraulic fractured coalbed methane recovery by thermal stimulation. In: SPE/CSUR Unconventional Resources Conference. Society of Petroleum Engineers. SPE 175927.

Wang Z.F., Li X.H., Qi L.L., The Study of the Moisture Effect on Gas Desorption Speed of Yangquan Anthracite. Mining Safety, 2010, 429(7), 1-3.

Xiao Z.H., Wang Z.F., 2011. Experimental study on inhibitory effect of gas desorption by injecting water into coal-sample. Procedia Eng, 26, 1287–1295.

Xie J.L., Zhao Y.S., Li X.C., 2011. The experiment of gas adsorption and desorption under the action of high temperature and high pressure water. Procedia Eng,26, 1547–1553.

Yahya, N., Kashif, M., Nasir, N., Akhtar, M.N., Yusof, N.M., 2012. Cobalt ferrite nanoparticles: an innovative approach for enhanced oil recovery application. J. Nano Res. 17, 115-126.

Zhang D.F., Cui Y.J., Li S.G., Song W.L., Lin W.G., 2011. Adsorption and diffusion behaviors of methane and carbon dioxide on various rank coals. J China Coal Soc, 35, 1963–1968.

Zhang Y.S., Sang S.X., 2009. Physical chemistry mechanism of influence of liquid water on coalbed methane adsorption. Procedia Earth Planet Sci, 1, 263–268.

Zhao D., Feng Z., Zhao Y., 2011. Laboratory experiment on coalbed-methane desorption influenced by water injection and temperature. J Can Pet Technol, 50, 24–33.

Zhou, F.B., Xia, T.Q., Wang, X.X., Zhang, Y.F., Sun, Y.N., Liu, J.S., 2016. Recent developments in coal mine methane extraction and utilization in China: a review. J. Nat. Gas Sci. Eng. 31, 437-458.

Fig.1   Experimental apparatus and coal samples used in these experiments

(The left is experimental apparatus, the middle is Coal sample 1# and the right is coal sample 2#.)
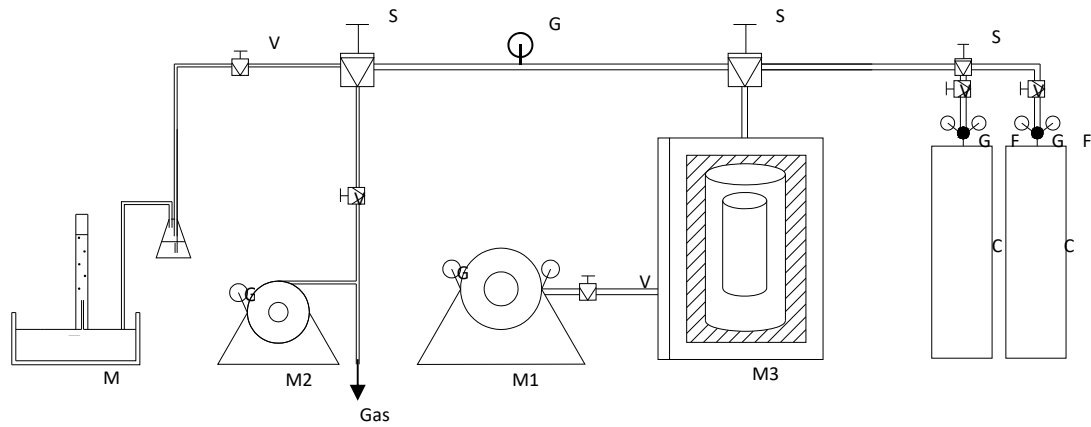
Fig.2 Schematic diagram of experimental apparatus used in this study.

(C1, C2: methane(CH₄) and helium(He) cylinder storage; F1, F2: flow of gas; G1, G2 or G3: gauge for displaying the pressure of methane, helium and water; G4: negative gauge for air pressure used for vacuum; G5: gauge for sample gas pressure; V1, V2, V3, V4 or V5: needle valves; S1, S2 or S3: three-port valves; M1: water injection pump; M2: vacuum pump; M3: temperature-controlling device; M4: measurement system.)
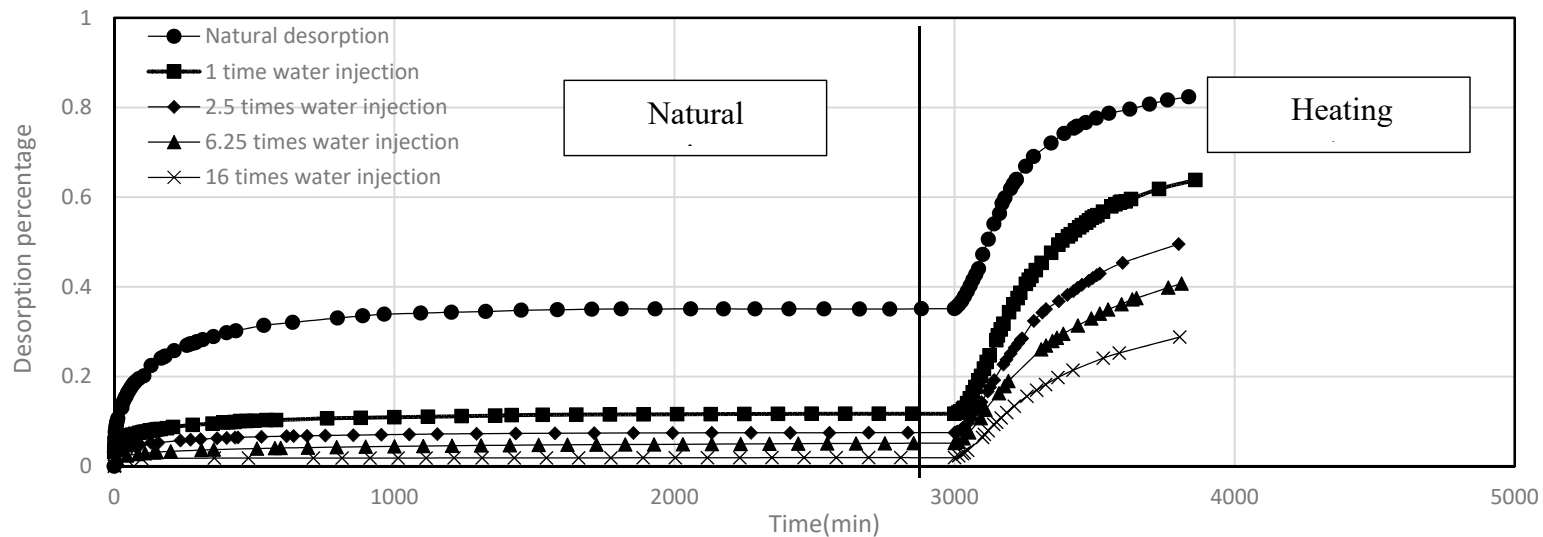
(a) Coal sample 1# (Gucheng Coal Mine)
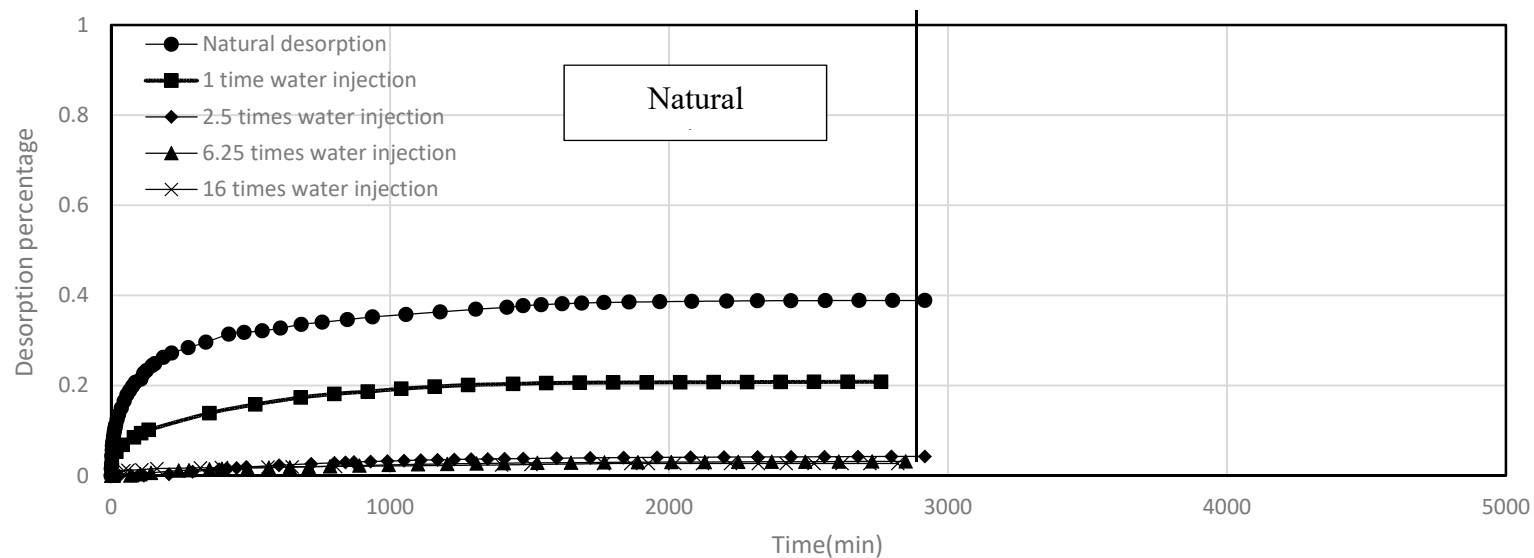
(b) Coal sample 2# (Gaohe Coal Mine)

Fig.3   Desorption capacity versus time in different water injection pressure at 0.25MPa gas adsorption pressure
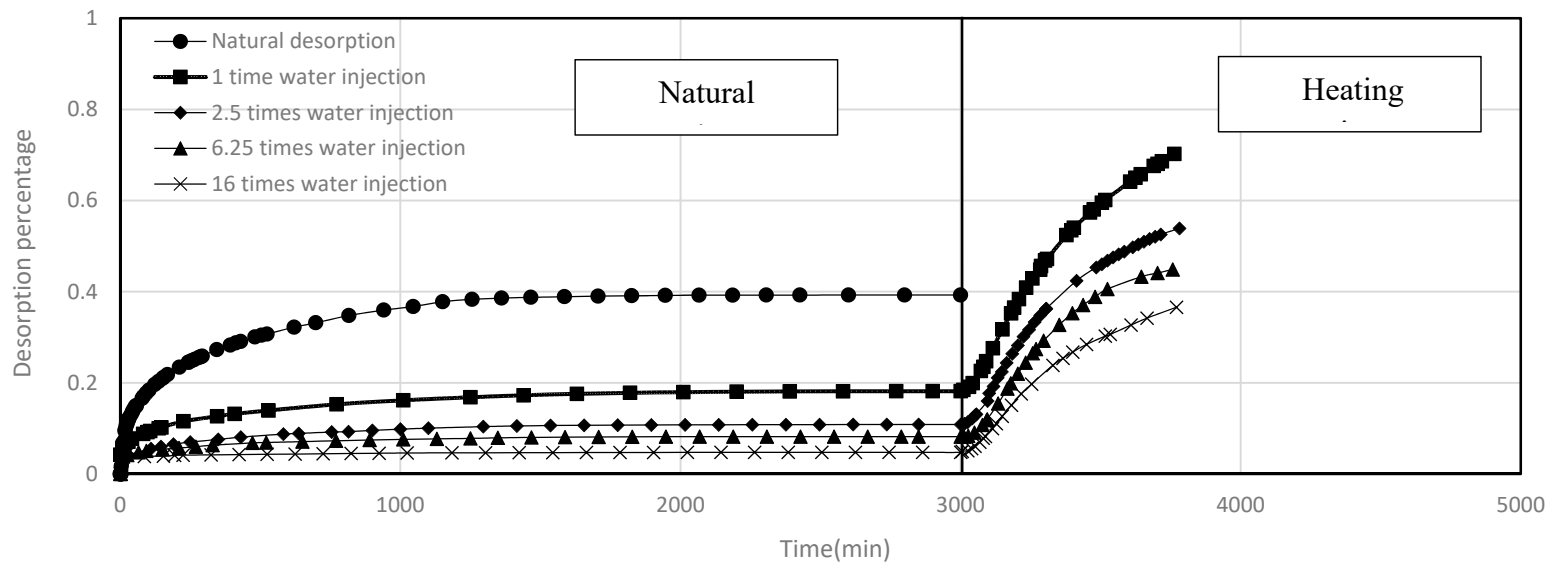
(a) Coal sample 1# (Gucheng Coal Mine)
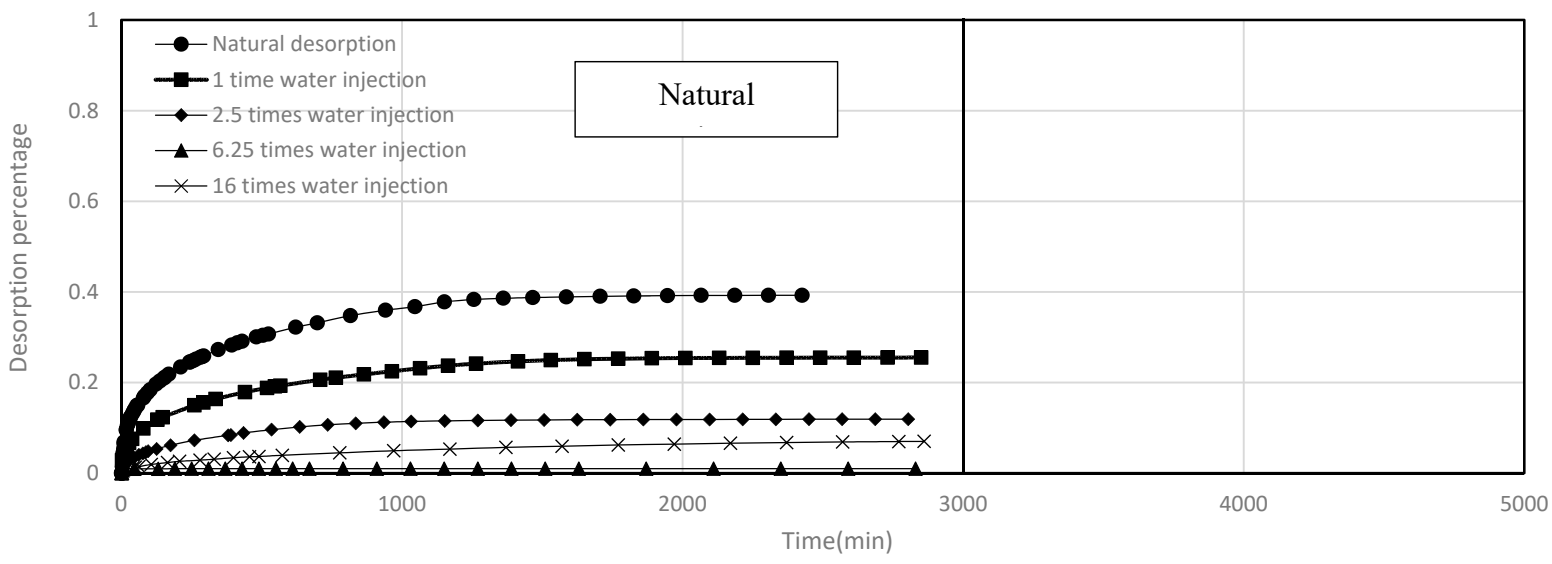
(b) Coal sample 2# (Gaohe Coal Mine)

Fig.4   Desorption capacity versus time in different water injection pressure around 0.50MPa gas adsorption pressure
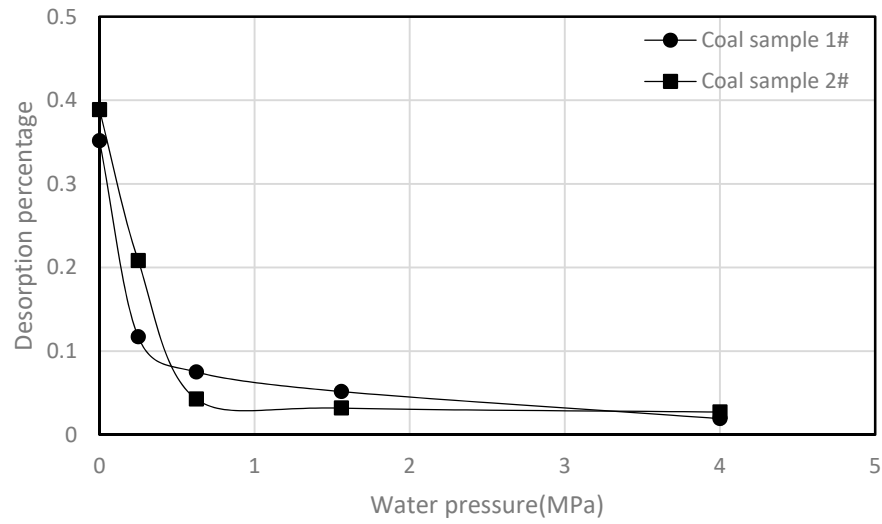
Fig.5　Desorption capacity as a function of water pressure for the two coal
samples at 0.25MPa gas adsorption pressure
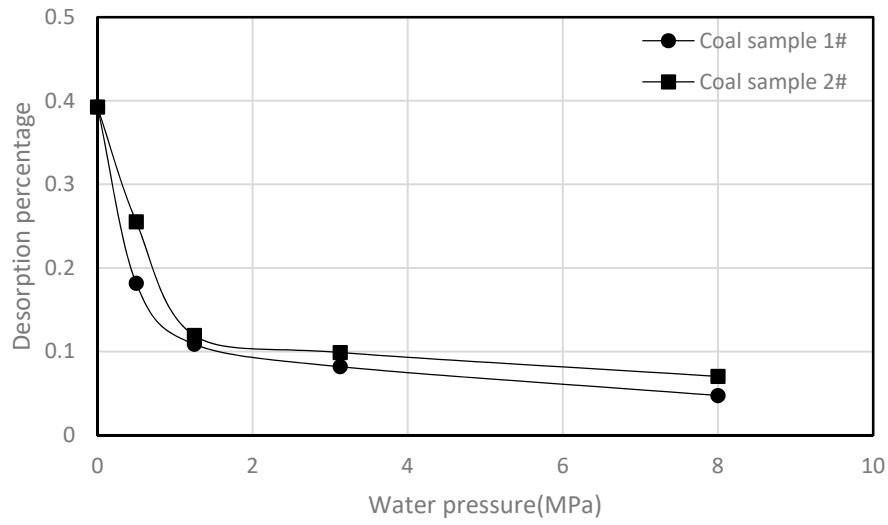
Fig.6   Desorption capacity as a function of water pressure for the two coal
samples at 0.50MPa gas adsorption pressure
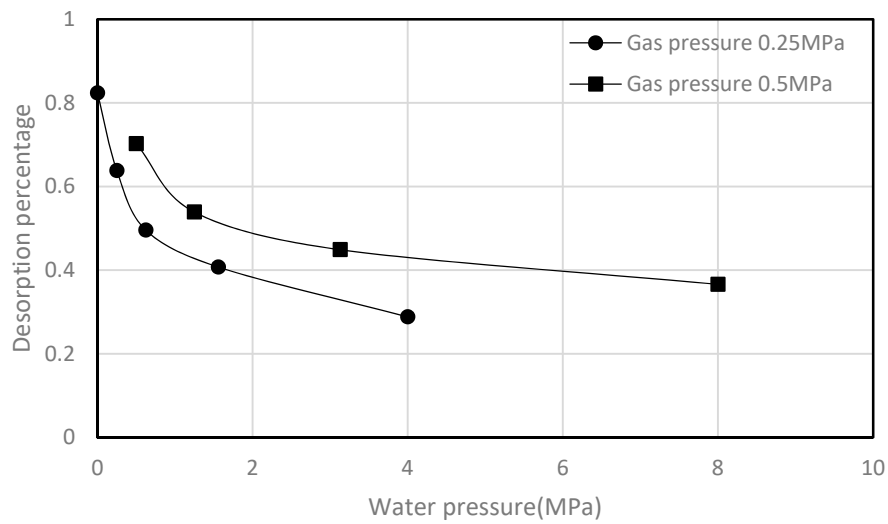
Fig.7 Desorption capacity as a function of water pressure at 90 ℃ for coal
sample 1#
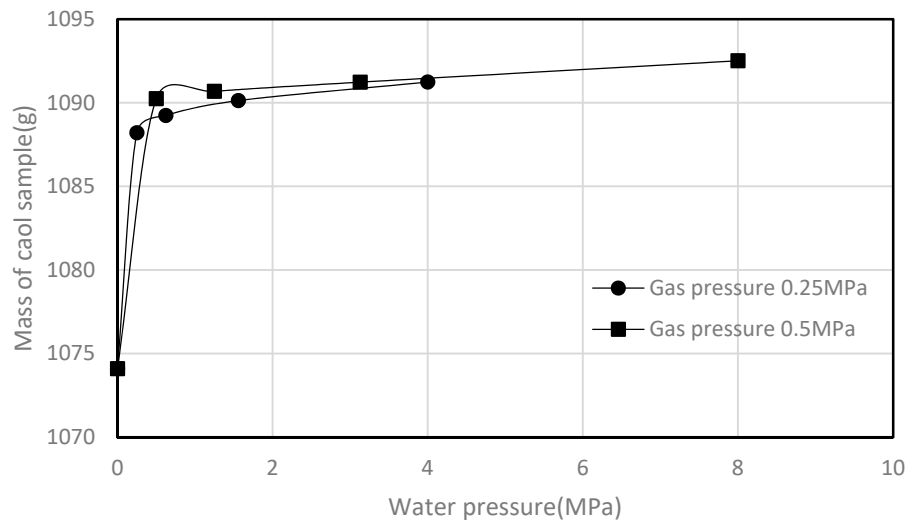
Fig.8 Mass of coal sample as a function of water pressure after desorption for
coal sample 2#

(The initial mass of coal sample is 1074.1g before experiment)

Table 1 Analysis results of experimental coal

Name of coal samples	R_{omax}(%)	M_{ad}(%)	A_d(%)	the volatile matter content	
				V_{ad}(%)	V_{daf}(%)
Gucheng (1#)	2.26	1.05	10.14	11.82	13.35
Gaohe (2#)	2.02	1.08	8.69	14.02	15.52

R_{omax}—vitrinite reflectance

M_{ad}—moisture content

A_d—ash content

V_{ad}—air drying base-volatile matter content

V_{daf}—dry ash-free basis volatile matter content

Table.2 Raw data of the two coal samples at gas adsorption pressure around 0.25MPa

Experimental Stage	Sample No.	ΔP/MPa	P_1/MPa	V_1/L	P_2/MPa	m_1/g	m_2/g	ω/%	V_2/L	V_3/L	V_4/L	dV_5/(ml/g)	η_{max}
Natural desorption	1#	0.11	0.295	1702	\	1101	\	0	93.62	272.63	4110.87	3.73	0.3477
	2#	0.11	0.241	1782.03	\	1074	\	0	102.02	242.73	4140.77	3.65	0.3717
1 time of adsorption pressure (about 0.25MPa)	1#	0.1	0.215	630	0.222	1101	\	1.455	93.86	199.21	3785.79	3.43	0.114
	1₂#	0.1	0.215	2400.68	0.222	1101	1117.02	1.455	93.86	199.21	3785.79	3.43	0.5815
	2#	0.11	0.230	1116.07	0.230	1074	1090.93	1.576	113.15	256.9	4126.6	3.84	0.2082
2.5 times of adsorption pressure (about 0.625MPa)	1#	0.1	0.195	401.57	0.508	1101	\	1.144	94.52	181.96	3803.04	3.45	0.0577
	1₂#	0.1	0.195	1269	0.508	1101	1112.66	1.144	94.52	181.96	3803.04	3.45	0.2858
	2#	0.105	0.182	441.14	0.458	1074	1089.24	1.41	101.95	183.18	4001.07	3.72	0.0644
6.25 times of adsorption pressure (about 1.56MPa)	1#	0.1	0.225	365.29	1.25	1101	\	1.57	93.81	208.38	3776.62	3.42	0.0415
	1₂#	0.1	0.225	1343	1.25	1101	1118.35	1.57	93.81	208.38	3776.62	3.42	0.3004
	2#	0.11	0.196	311.4	1.295	1074	1090.13	1.502	102.02	197.41	4186.09	3.89	0.0272
16 times of adsorption pressure (about 4.00MPa)	1#	0.1	0.215	269.02	3.212	1101	\	1.251	93.861	199.21	3785.79	3.43	0.0192
	1₂#	0.1	0.215	1018	3.212	1101	1114.77	1.251	93.861	199.21	3785.79	3.43	0.2162
	2#	0.11	0.195	211.36	3.223	1074	1091.24	1.605	102.02	196.40	4187.1	3.89	0.0271

Note: ΔP means D-value between initial and final gas pressure of gas storage tank, which the content is 3.8L; P_1 means gas adsorption pressure at final stage; V_1 means desorption volume of coal sample at each stage; P_2 means water injection pressure, it is depends on final gas adsorption pressure; V_2 means free content after coal into sample container, it is measured by Helium; m_1 means the mass of dry coal sample; m_2 means the mass of wet coal sample after water injection and desorption; ω is the moisture content of the coal sample appending on dry coal after water injection and desorption; V_3 and V_4 are free gas volume and adsorption gas volume, respectively; dV_5 means adsorption gas volume per unit mass of coal; and η_{max} is accumulative desorption rate after 48h desorption. All data is converted to the value at standard status (273.15 K, 1 atm).

Table.3 Raw data of the two coal samples at gas adsorption pressure around 0.50MPa

Experimental Stage	Sample No.	ΔP/MPa	P_1/MPa	V_1/L	P_2/MPa	m_1/g	m_2/g	ω/%	V_2/L	V_3/L	V_4/L	dV_5/(ml/g)	η_{max}
Natural desorption	1#	0.2	0.459	3349	\	1101	\	0	93.64	424.32	7545.67	6.85	0.3875
	2#	0.22	0.506	4432	\	1074	\	0	101.73	508.15	8258.84	7.68	0.4751
1 time of adsorption pressure (about 0.25MPa)	1#	0.18	0.535	1702.8	0.53	1101	\	1.303	93.86	495.71	6677.28	6.06	0.1807
	1₂#	0.18	0.535	4420	0.53	1101	1115.3	1.303	93.86	495.71	6677.28	6.06	0.5878
	2#	0.2	0.505	2354.4	0.52	1074	1090.2	1.512	102.02	508.63	7461.36	6.94	0.2473
2.5 times of adsorption pressure (about 0.625MPa)	1#	0.185	0.528	1129.8	1.32	1101	\	1.265	93.86	489.22	6883.02	6.25	0.0930
	1₂#	0.185	0.528	4855	1.32	1101	1114.9	1.265	93.86	489.22	6883.02	6.25	0.7984
	2#	0.2	0.486	1281.2	1.23	1074	1090.6	1.553	102.02	489.49	7480.50	6.96	0.1058
6.25 times of adsorption pressure (about 1.56MPa)	1#	0.185	0.611	1007.9	3.82	1101	\	1.362	93.86	566.13	6606.86	6.00	0.0668
	1₂#	0.185	0.611	3596	3.82	1101	1116	1.362	93.86	566.13	6606.86	6.00	0.6111
	2#	0.2	0.5	979	3.12	1074	1092.6	1.732	84.73	418.23	7551.76	7.03	0.0742
16 times of adsorption pressure (about 4.00MPa)	1#	0.185	0.495	700.31	8	1101	\	1.306	93.86	458.65	6714.34	6.09	0.0474
	1₂#	0.185	0.495	3617.3	8	1101	1115.3	1.306	93.86	458.65	6714.34	6.09	0.47
	2#	0.2	0.488	944.65	8	1074	1092.5	1.723	102.02	491.51	7478.48	6.96	0.0556

Table 4   Simulation results of time effect on desorption

Sample No.	Adsorption gas pressure	Experimental stage	Simulation results from Equation (1)	Results from Equation (2)	R^2
1#	0.25MPa	Natural desorption	$\eta=\eta_{max}\{1-exp[-(t/_{0.01055})^{0.5393}]\}$	$y=0.0859x^{0.5393}$	0.9735
		1 time	$\eta=\eta_{max}\{1-exp[-(t/_{0.017144})^{0.365}]\}$	$y=0.2267x^{0.365}$	0.8843
		2.5times	$\eta=\eta_{max}\{1-exp[-(t/_{0.019.34})^{0.3743}]\}$	$y=0.227x^{0.3743}$	0.9244
		6.25times	$\eta=\eta_{max}\{1-exp[-(t/_{0.00706})^{0.1796}]\}$	$y=0.0256x^{0.1796}$	0.9933
		16times	$\eta=\eta_{max}\{1-exp[-(t/_{0.00586})^{0.1079}]\}$	$y=2.7378x^{0.1079}$	0.9131
1#	0.50MPa	Natural desorption	$\eta=\eta_{max}\{1-exp[-(t/_{0.005252})^{0.6349}]\}$	$y=0.0357x^{0.6349}$	0.9617
		1 time	$\eta=\eta_{max}\{1-exp[-(t/_{0.007177})^{0.493}]\}$	$y=0.0877x^{0.493}$	0.9261
		2.5times	$\eta=\eta_{max}\{1-exp[-(t/_{0.005283})^{0.5988}]\}$	$y=0.0443x^{0.5988}$	0.9534
		6.25times	$\eta=\eta_{max}\{1-exp[-(t/_{0.016739})^{0.3604}]\}$	$y=0.229x^{0.3604}$	0.8997
		16times	$\eta=\eta_{max}\{1-exp[-(t/_{0.086339})^{0.2769}]\}$	$y=0.5075x^{0.2769}$	0.8695
2#	0.25MPa	Natural desorption	$\eta=\eta_{max}\{1-exp[-(t/_{0.00708})^{0.5592}]\}$	$y=0.0628x^{0.5592}$	0.9836
		1 time	$\eta=\eta_{max}\{1-exp[-(t/_{0.006066})^{0.5977}]\}$	$y=0.0473x^{0.5977}$	0.9464
		2.5times	$\eta=\eta_{max}\{1-exp[-(t/_{0.0011393})^{1.359}]\}$	$y=0.0001x^{1.359}$	0.9723
		6.25times	$\eta=\eta_{max}\{1-exp[-(t/_{0.001420})^{1.2372}]\}$	$y=0.0003x^{0.1.2372}$	0.9006
		16times	$\eta=\eta_{max}\{1-exp[-(t/_{0.007109})^{0.3814}]\}$	$y=0.1516x^{0.3814}$	0.8335
2#	0.50MPa	Natural desorption	$\eta=\eta_{max}\{1-exp[-(t/_{0.005252})^{0.6349}]\}$	$y=0.0357x^{0.6349}$	0.9617
		1 time	$\eta=\eta_{max}\{1-exp[-(t/_{0.005112})^{0.6054}]\}$	$y=0.041x^{0.6054}$	0.9536
		2.5times	$\eta=\eta_{max}\{1-exp[-(t/_{0.0054527})^{0.622}]\}$	$y=0.0391x^{0.622}$	0.9611
		6.25times	$\eta=\eta_{max}\{1-exp[-(t/_{0.001430})^{1.0708}]\}$	$y=0.0009x^{1.0708}$	0.9475
		16times	$\eta=\eta_{max}\{1-exp[-(t/_{0.006566})^{0.512}]\}$	$y=0.0026x^{0.512}$	0.9164

Table 5 **Simulation results between desorption percentage and water injection pressure**

Sample No.	Adsorption gas pressure	Simulation results of Equation (3)	Simulation results of Equation (4)	R^2
1#	0.25MPa	$\eta_{max}=\eta_{d\,max}$ $(1-2.2492P_4/（1+2.1641P_4）)$	y=0.4446x+1.0393	0.9896
2#	0.50MPa	$\eta_{max}=\eta_{d\,max}$ $(1-0.7251P_4/（1+0.6699P_4）)$	y=1.379x+1.0824	0.9591
1#	0.25MPa	$\eta_{max}=\eta_{d\,max}$ $(1-1.2318P_4/（1+1.1777P_4）)$	y=0.8118x+1.0459	0.9877
2#	0.50MPa	$\eta_{max}=\eta_{d\,max}$ $(1-0.9689P_4/（1+0.9617P_4）)$	y=1.032x+1.0075	0.9565